JPET Fast Forward. Published on March 13, 2015 as DOI: 10.1124/jpet.114.221861
This article has not been copyedited and formatted. The final version may differ from this version.

JPET #221861

Ranolazine reduces remodeling of the right ventricle and provoked arrhythmias in rats with pulmonary hypertension

John T. Liles[#], Kirsten Hoyer[#], Jason Oliver, Liguo Chi, Arvinder K. Dhalla, and Luiz Belardinelli

Department of Biology, Gilead Sciences, Inc.

Downloaded from jpet.aspetjournals.org at ASPET Journals on December 28, 2024

[#]See footnote.

JPET Fast Forward. Published on March 13, 2015 as DOI: 10.1124/jpet.114.221861
This article has not been copyedited and formatted. The final version may differ from this version.

a) Running title: Ranolazine reduces cardiac remodeling in PAH rats

b) Kirsten Hoyer, Gilead Sciences Inc., 7601 Dumbarton Circle, Fremont, CA 94555

phone: 510.739.8434

fax: 510.739.8403

e-mail: kirsten.hoyer@gilead.com

c) number of text pages: 20

number of tables: 2

number of figures: 7

number of references: 39

number of words - Abstract: 220

Introduction: 748

Discussion: 1469

d) List of nonstandard abbreviations

APD	action potential duration
BNP	B-type natriuretic peptide
CTGF	connective tissue growth factor
dPAP	diastolic pulmonary arterial pressure
ERP	effective refractory period
HF	heart failure
I_{Na}	sodium current

Downloaded from jpet.aspetjournals.org at ASPET Journals on December 28, 2024

JPET Fast Forward. Published on March 13, 2015 as DOI: 10.1124/jpet.114.221861
This article has not been copyedited and formatted. The final version may differ from this version.

ISO	isoproterenol
LVP	left ventricular pressure
LVSP	left ventricular systolic pressure
MAP(D)	monophasic action potential (duration)
MCT	monocrotaline
mPAP	mean pulmonary arterial pressure
PAH	pulmonary arterial hypertension
PVR	pulmonary vascular resistance
QTc	heart-rate corrected QT
RAN	ranolazine
RV	right ventricle
SCD	sudden cardiac death
sPAP	systolic arterial pressure
TGF-β	transforming growth factor- β
TL	tibia length
VT/VF	ventricular tachycardia/ventricular fibrillation

e) Cardiovascular

Downloaded from jpet.aspetjournals.org at ASPET Journals on December 28, 2024

JPET Fast Forward. Published on March 13, 2015 as DOI: 10.1124/jpet.114.221861
This article has not been copyedited and formatted. The final version may differ from this version.

Abstract

Pulmonary arterial hypertension (PAH) is a progressive disease that often results in right ventricular (RV) failure and death. During disease progression, structural and electrical remodeling of the RV impairs pump function, creates pro-arrhythmic substrates and triggers for arrhythmias. Notably, RV failure and lethal arrhythmias are major contributors to cardiac death in patients with PAH that are not directly addressed by currently available therapies. Ranolazine (RAN) is an anti-anginal, anti-ischemic drug that has cardioprotective effects in experimental and clinical settings of left-sided heart dysfunction. RAN also has anti-arrhythmic effects due to inhibition of the late sodium current in cardiomyocytes. We therefore hypothesized that RAN could reduce the maladaptive structural and electrical remodeling of the RV, and prevent triggered ventricular arrhythmias in the monocrotaline rat model of PAH. Indeed, in both *in vivo* and *ex vivo* experimental settings, chronic RAN treatment reduced electrical heterogeneity (RV-LV APD dispersion) and shortened QTc intervals in the RV, and normalized RV dysfunction. Chronic RAN also dose-dependently reduced ventricular hypertrophy, reduced circulating levels of BNP, and decreased the expression of fibrotic markers. In addition, the acute administration of RAN prevented isoproterenol-induced VT/VF and subsequent cardiovascular death in rats with established PAH. These results support the notion that RAN can improve the electrical and functional properties of the RV, highlighting its potential benefits in the setting of RV impairment.

Downloaded from jpet.aspetjournals.org at ASPET Journals on December 28, 2024

JPET Fast Forward. Published on March 13, 2015 as DOI: 10.1124/jpet.114.221861
This article has not been copyedited and formatted. The final version may differ from this version.

Introduction

Pulmonary arterial hypertension (PAH) is a progressive and fatal disease characterized by vascular remodeling and vasoconstriction of the pulmonary arterial circulation that often results in right ventricular (RV) failure and death. The progressive vasculopathy leads to intraluminal narrowing and obstruction of the resistance vasculature leading to sustained increases in pulmonary vascular resistance (PVR) and pulmonary arterial pressure. In an attempt to compensate for the increased afterload and wall stress, the RV undergoes structural and electrical remodeling (Malenfant et al., 2013; Simon, 2013), creating pro-arrhythmic substrates and triggers for arrhythmias (Benoist et al., 2011; Benoist et al., 2012; Rocchetti et al., 2014). Although the extent of the vascular pathology in PAH can determine morbidity and mortality, RV dysfunction is now recognized as the key determinant of disease outcome (Voelkel et al., 2012; Archer et al., 2013; Rain et al., 2013; Rain et al., 2014). The central role of RV pathology in disease progression is underscored by evidence showing that RV failure is the primary cause of death in patients with PAH, and by reports that lethal arrhythmias are a major contributor to sudden cardiac death (SCD) in these patients (Rajdev et al., 2012; Voelkel et al., 2012; Olsson et al., 2013; Rain et al., 2013; Rich et al., 2013; Rain et al., 2014).

Current PAH therapies, consisting mainly of prostanoids, phosphopdiesterase type-5 inhibitors, and endothelin receptor antagonists, reduce PVR through preferential vasodilation of the pulmonary circulation (Abraham et al., 2010; van de Veerdonk et al., 2011). This strategy of targeting the vasoconstrictive component of PAH improves symptoms and slows disease progression, but mortality rates remain high and functional impairment of RV function remains a significant problem (van de Veerdonk et al., 2011; Archer et al., 2013; Guihaire et al., 2013;

Downloaded from jpet.aspetjournals.org at ASPET Journals on December 28, 2024

JPET Fast Forward. Published on March 13, 2015 as DOI: 10.1124/jpet.114.221861
This article has not been copyedited and formatted. The final version may differ from this version.

Malenfant et al., 2013; Rain et al., 2013). There is no current PAH therapy that directly targets the structural and electrical consequences of RV remodeling (Archer et al. 2013, Olsson et al., 2013, Voelkel et al., 2012).

Ranolazine (RAN), is an FDA-approved anti-anginal drug with anti-ischemic activity that has also been shown to have anti-arrhythmic properties due to inhibition of the late sodium current (I_{Na}) in cardiomyocytes (Hale et al., 2008; Antzelevitch et al., 2014). As a result of extensive clinical and experimental studies, the cardioprotective effects of RAN in settings of left-sided heart dysfunction are well established (Rastogi et al., 2008; Aistrup et al., 2013; Maier et al., 2013). Although the LV and RV have notable and well-defined differences (i.e. structural, functional, electrical, and embryological), common mechanisms such as ischemia, Ca^{2+} overload, oxidative stress, and fibrosis are implicated in the pathology of both left- and right-sided HF (Bogaard et al., 2009; Borgdorff et al., 2013; Simon, 2013; Toischer et al., 2013). Pathological processes which are known to increase late I_{Na} (Voelkel et al., 2012; Freund-Michel et al., 2013; Shryock et al., 2013; Toischer et al., 2013) are also implicated in the progression of RV failure in PAH (Voelkel et al., 2012; Freund-Michel et al., 2013; Shryock et al., 2013; Toischer et al., 2013). However, it was recently reported that RAN reduced RV mass, improved RV performance, and increased exercise capacity in 10 patients with WHO Group 1 PAH and symptoms of angina (Shah et al., 2012). It has also been reported that RAN can reduce RV hypertrophy in a rat model where RV pressure-overload is induced independently from changes in pulmonary arterial pressures by pulmonary artery banding (Fang et al., 2012). Additionally, a recent study in a 3 week MCT rat model showed that RAN, when initiated 2 days after MCT injection, prevented RV structural and electrical remodeling by suppressing late I_{Na} (Rocchetti et

Downloaded from jpet.aspetjournals.org at ASPET Journals on December 28, 2024

JPET Fast Forward. Published on March 13, 2015 as DOI: 10.1124/jpet.114.221861
This article has not been copyedited and formatted. The final version may differ from this version.

al., 2014). MCT is known to consistently induce pulmonary vascular remodeling in the rat within the first 4-7 days following injection, with peak increases in pulmonary pressure occurring at 4-5 weeks (Bruner et al., 1983; Rosenberg and Rabinovitch, 1988; Hoorn and Roth, 1992; Lappin and Roth, 1997; Guihaire et al., 2013).

In our study, RAN treatment was started at day 7 following MCT injection to allow for the vasculopathy to develop prior to intervention, and all endpoints were assessed 4 weeks following MCT. We used a combination of *in vivo* and *ex vivo* approaches to determine if treatment with RAN could halt the development of the PAH phenotype in a model that reliably reproduces RV impairment and major pathological features of the human disease, and to extend recent findings by determining if RAN treatment prevents the induction of arrhythmias/SCD in rats with established PAH.

Downloaded from jpet.aspetjournals.org at ASPET Journals on December 28, 2024

JPET Fast Forward. Published on March 13, 2015 as DOI: 10.1124/jpet.114.221861
This article has not been copyedited and formatted. The final version may differ from this version.

Materials and Methods

Animals. Male Sprague-Dawley rats (250-300 g, Hollister, CA) were used in this study. Experiments were performed under protocols approved by the Institutional Animal Care and Use Committee of Gilead Sciences (AAALAC International Accreditation Number, 001135). Animal use conformed to the guidelines of National Institutes of Health (NIH publication no. 85-23, revised 1996). Animals received a single subcutaneous injection of monocrotaline (MCT, 60 mg/kg body weight) to induce pulmonary arterial hypertension (PAH) within 28 days and control rats received an equal volume of solvent (vehicle, 1 mL/kg body weight). All animals had free access to standard rodent chow (Nestle, CH) and water for the first week post MCT injection, thereafter subsets of rats were switched to a diet containing either 0.25% ranolazine (0.25% RAN) or 0.5% ranolazine (0.5% RAN) by weight to determine the effect of chronic RAN administration during PAH development (Research Diets, New Brunswick, NJ). Plasma levels of RAN achieved in the present study using chronic oral administration (0.25% = 1-2 μM, 0.5%= 4-7 μM) are within the therapeutic range (6-8 μM). At these concentrations RAN selectively inhibits late I_{Na} versus other targets (Hale et al., 2008; Zhao et al., 2011).

For the *in vivo* studies, rats were divided into four groups that received (a) vehicle injection and normal diet (sham), (b) MCT injection and normal diet (PAH), (c) MCT injection and diet containing 0.25% RAN, and (d) MCT injection and diet containing 0.5% RAN.

Rats used in the *ex vivo* studies (isolated heart) were separated into four treatment groups: (a) vehicle injection and normal diet (sham), (b) vehicle injection and diet containing 0.5% Ran (sham+0.5% RAN), (c) MCT injection and normal diet (PAH), and (d) MCT injection and diet containing 0.5% Ran (PAH+0.5% RAN). For all studies, Purina #5001 was used as the standard

Downloaded from jpet.aspetjournals.org at ASPET Journals on December 28, 2024

JPET Fast Forward. Published on March 13, 2015 as DOI: 10.1124/jpet.114.221861
This article has not been copyedited and formatted. The final version may differ from this version.

rodent chow, and the only difference between diets was the concentration of RAN (0% for sham and PAH, 0.25%, or 0.5% by weight for respective experiments).

***In Vivo* Measurements.** At 4 weeks post MCT administration, rats were anesthetized using isoflurane (Sigma-Aldrich, St. Louis, MO), then intubated and ventilated. Body temperature was measured using a rectal thermometer and was maintained at 37ºC using a heating pad. After a stabilization period, pulmonary hemodynamics were assessed using a Millar catheter (SPR-839, Millar Instruments, TX) inserted into the right ventricle (RV) and advanced into the pulmonary artery. Thereafter, the same SPR-839 catheter was slowly pulled back into the RV to also acquire RV hemodynamics. A separate Millar catheter (SPR-869) was inserted into the right common carotid artery for measurement of systemic arterial pressure. After allowing for stabilization from surgical preparation, data was continuously recorded on a personal computer using a pressure-volume unit (model MPVS-300; ADInstruments, Colorado Springs, CO). Additionally, an electrocardiogram (ECG) was recorded using subdermal needle electrodes (25 gauge, ADInstruments, Colorado Springs, CO) in the lead II configuration.

BNP (AbCam Inc. cat #ab108816) protein analysis in plasma was performed according to the manufacturer's instructions. In brief, a 1:4 fold dilution and 1:10 fold dilution of plasma for BNP and TIMP-1, respectively, were incubated for 2 hours at room temperature using manufacture's assay reagents. Both BNP and TIMP-1 protein concentrations were calculated from their assay standard curve OD values.

Tissue Collection and Morphological Measurements. At the conclusion of hemodynamic procedures, rats were sacrificed so that blood and organs could be collected for further evaluation. The heart was dissected into atria, RV, and LV (including the septum), plotted dry

Downloaded from jpet.aspetjournals.org at ASPET Journals on December 28, 2024

JPET Fast Forward. Published on March 13, 2015 as DOI: 10.1124/jpet.114.221861
This article has not been copyedited and formatted. The final version may differ from this version.

with gauze and weighed. RV hypertrophy was determined by the ratio of RV weight divided by tibia length (RV/TL). This measurement has the advantage of being unaffected by body weight and LV mass changes (Yin et al., 1982).

Measurements of Fibrosis and Inflammation Markers. Paraffin-embedded cross sections (5μm) of RV were prepared from paraformaldehyde-fixed tissues and stained with Masson's Trichrome for tissue collagen and then imaged. The mRNA gene expression of collagen 1α1, connective tissue growth factor (CTGF) and transforming growth factor-β (TGF-β) in RV tissue was determined using Luminex xMap technology according to manufacturer's instructions (Luminex Inc., Austin, TX). Briefly, approximately 50 mg of tissue was lysed in homogenizing buffer (Affymetrix Inc., Santa Clara, CA) and then incubated with mRNA detection probe panel (Affymetrix Inc., Santa Clara, CA) at 54^{o}C overnight. On the following day, tissue lysates and mRNA detection probe cocktail was hybridized with amplifier reagents in accordance to manufacture instructions. Data were collected using laser-detected Luminex SD equipment and analyzed by Masterplex CT software (Luminex Inc., Austin, TX).

Langendorff Perfusion. At 28 days post MCT injection rats were anesthetized (60 mg/kg ketamine/xylazine, i.p.), hearts isolated, and mounted on a Langendorff perfusion system and perfused at constant pressure (70 mmHg) with Krebs-Henseleit buffer containing (in mM): 118 NaCl, 25 $NaHCO_3$, 11 glucose, 4.2 KCl, 1.2 KH_2PO_4, 1.2 $MgSO_4$, 0.5 EDTA, and 1.5 $CaCl_2$. The buffer was continuously gassed with 95% O_2-5% CO_2 (pH 7.4) at 37ºC. The effluent of the *Thebesian* veins was drained via polyethylene tubing (PE-50) placed at the left ventricular (LV) apex. Isovolumic contractile performance was measured using a water-filled balloon inserted

Downloaded from jpet.aspetjournals.org at ASPET Journals on December 28, 2024

JPET Fast Forward. Published on March 13, 2015 as DOI: 10.1124/jpet.114.221861
This article has not been copyedited and formatted. The final version may differ from this version.

into the LV (for more information see supplemental data). Hearts were paced at 5 Hz using a bipolar electrode placed on the epicardial wall of the right ventricle and connected to a stimulator (S88 stimulator, Grass, Warwick, RI).

Measurements of Electrophysiological Parameters in the Isolated Heart. Pseudo ECGs were obtained with Ag-AgCl monopolar ECG electrodes (Harvard Apparatus, Holliston, MA) and the heart-rate corrected QT (QTc) intervals were calculated according to the Bazett formula. Monophasic action potentials (MAPs) were recorded at the epicardial surfaces of the LV and RV using pressure-contact Mini MAP electrodes (Harvard Apparatus, Holliston, MA). MAP duration (MAPD) was measured at 30, 50, and 90% repolarization. The interventricular dispersion of repolarization was defined as RV minus LV $MAPD_{90}$. The ventricular effective refractory period (ERP) was determined as the shortest S1-S2 interval generating an MAP by stimulating hearts using an S1-S2 protocol: S1 pulses were continuously applied at an interval of 200 ms and an S2 stimulus was introduced at various coupling intervals that were reduced from 100 to 50 ms at 10 ms decrements and from 48 to 30 ms at 2 ms decrements.

To trigger ventricular arrhythmia hearts paced at 6 Hz underwent burst pacing (50 Hz for 1 second) at which time the electrical pacing was stopped to allow the heart to resume its intrinsic rate. Stimulus intensity during burst pacing was increased until tachycardia or fibrillation was induced (Benoist et al., 2011).

Induction of Arrhythmias in PAH Rats and Isolated Hearts during Acute Ranolazine Treatment. In *in vivo* experiments cardiac arrhythmia was induced with isoproterenol (ISO, 0.1 mg/kg, i.v.; ISO challenge) in a group of rats post 49 – 60 days MCT or vehicle injection. To

Downloaded from jpet.aspetjournals.org at ASPET Journals on December 28, 2024

JPET Fast Forward. Published on March 13, 2015 as DOI: 10.1124/jpet.114.221861
This article has not been copyedited and formatted. The final version may differ from this version.

determine the acute anti-arrhythmic effect of RAN, a subgroup rats with PAH received RAN (8 mg/kg bolus, followed by 10mg/kg/h infusion, i.v.) 10 min prior to the ISO challenge.

In isolated hearts from rats with established PAH arrhythmia was provoked with the above mentioned burst pacing protocol (50 Hz, 1 s, increasing stimulus intensity). Ten rat hearts were treated with 10 μM RAN 10 min prior to and during the burst pacing protocol.

Data were acquired on a Power Lab 8/30 (ADInstruments, Colorado Springs, CO) attached to a computer and was analyzed with LabChart Pro7 software (ADInstruments, Colorado Springs, CO).

Chemicals. Ranolazine was provided by Gilead Sciences Inc. All other reagents including monocrotaline were obtained from Sigma-Aldrich (St. Louis, MO).

Statistics. All data are expressed as mean ± S.E.M. Statistical analyses were performed using one-way analysis of variance (one-way ANOVA) followed by either the Newman-Keuls post-hoc test or Tukey post-hoc test for multiple comparisons. The Fisher's exact test was used for analyzing the differences in the incidences of arrhythmias (GraphPad Prism 6.00, GraphPad Software, La Jolla, CA). Value of $P < 0.05$ was considered statistically significant.

Downloaded from jpet.aspetjournals.org at ASPET Journals on December 28, 2024

JPET Fast Forward. Published on March 13, 2015 as DOI: 10.1124/jpet.114.221861
This article has not been copyedited and formatted. The final version may differ from this version.

Results

Chronic Administration of Ranolazine Reduces MCT-induced RV Hypertrophy and Normalizes RV Performance. The effect of 0.25 and 0.5% RAN in diet on RV hypertrophy, RV developed pressure (mmHg), and plasma levels of B-type natriuretic peptide (BNP; pg/ml) in MCT rats, are summarized in figure 1. At 4 weeks, as expected, MCT administration caused RV hypertrophy (9.8 ± 0.8 vs. 6.2 ± 0.1 mg/mm, RV/TL), increased RV developed pressure (68 ± 7 vs. 24 ± 0.3 mmHg), and increased plasma BNP levels three-fold (527 ± 113 vs. 173 ± 89 pg/ml) when compared to sham controls (Fig. 1). Chronic treatment with RAN (0.25 and 0.5%), starting at 1 week following the administration of MCT, dose-dependently reduced RV hypertrophy (7.8 ± 0.7 and 5.7 ± 0.3 mg/mm), developed pressure (51 ± 6 and 34 ± 2 mmHg), and BNP plasma levels (266 ± 114 and 57 ± 17 pg/ml). RAN had no effect on systemic blood pressure or heart rate (Table 1).

Chronic Administration of Ranolazine Reduces MCT-induced PAH. Pulmonary hemodynamic measurements were acquired directly from the proximal pulmonary artery using a solid-state catheter (Millar, SPR-839) at 4 weeks following MCT injection. MCT administration induced significant increases in systolic pulmonary arterial pressure (sPAP; 68 ± 6 vs. 23 ± 1 mmHg), mean pulmonary arterial pressure (mPAP; 40 ± 3 vs. 17 ± 1 mmHg), and diastolic pulmonary arterial pressure (dPAP; 22 ± 1 vs. 10 ± 1 mmHg) when compared to sham controls (Fig. 2). Chronic treatment with RAN (0.25 and 0.5%), starting at 1 week following the injection of MCT, dose-dependently reduced sPAP (53 ± 5 and 34 ± 1 mmHg), mPAP (32 ± 2 and 24 ± 1 mmHg), and dPAP (18 ± 1 and 15 ± 1 mmHg; Fig. 2).

Downloaded from jpet.aspetjournals.org at ASPET Journals on December 28, 2024

JPET Fast Forward. Published on March 13, 2015 as DOI: 10.1124/jpet.114.221861
This article has not been copyedited and formatted. The final version may differ from this version.

Chronic Administration of Ranolazine Reduces RV Collagen Deposition and Fibrotic Gene Expression. To evaluate the effect of RAN treatment on the development of cardiac fibrosis and remodeling, RV samples were collected 4 weeks following the injection of MCT for histology and gene expression patterns in the RV (Fig. 3). RV sections stained with Masson's Trichrome showed more pronounced collagen deposition from animals with PAH compared to sham and to animals treated with 0.5% RAN (Fig. 3A-C). RVs from rats with MCT-induced PAH had increased expression of the mRNA transcripts for collagen 1α1 (Fig. 3D), connective tissue growth factor (CTGF; Fig. 3E), and TGF-β (Fig. 3F). RAN dose-dependently reduced the expression of these fibrotic genes in the RV (Fig. 3D-F).

Chronic Administration of Ranolazine Reduces Electrical Remodeling in Hearts Isolated from Rats with PAH. Hearts were isolated 4 weeks following the injection of MCT from rats treated with vehicle (standard rodent chow) or 0.5% RAN, or from sham animals with and without RAN treatment. The effect of chronic treatment with RAN on the RV MAPD, the ventricular heterogeneity in repolarization (RV-LV $MAPD_{90}$), and EP parameters was determined, and these data are summarized in figures 4-5. Sham animals on standard chow had RV MAPDs of 17 ± 2.2 ms, 24 ± 2.8 ms and 50 ± 3.8 ms measured at 30%, 50% and 90% repolarization, respectively. RV $MAPD_{30}$ and $MAPD_{50}$ increased 2-fold in hearts from animals with PAH compared to sham (37 ± 1.7 vs. 17 ± 2.2 ms, 47 ± 3.5 vs. 24 ± 2.8 ms) and $MAPD_{90}$ increased 1.6-fold (83 ± 6.0 vs. 50 ± 3.8 ms; Fig. 4B). The prolongation of the MAPDs observed at 4 weeks following the injection of MCT was significantly less in hearts from rats with PAH treated with 0.5% RAN (23 ± 1.7, 31 ± 2.1, and 62 ± 3.5 ms for $MAPD_{30}$, $MAPD_{50}$, and $MAPD_{90}$, respectively).

Downloaded from jpet.aspetjournals.org at ASPET Journals on December 28, 2024

JPET Fast Forward. Published on March 13, 2015 as DOI: 10.1124/jpet.114.221861
This article has not been copyedited and formatted. The final version may differ from this version.

In addition, the interventricular dispersion in $MAPD_{90}$ was markedly increased in hearts from rats with PAH compared to the shams (17 ± 5.5 vs. -6.1 ± 2.0 ms), whereas RAN treatment normalized dispersion values (-2 ± 2.4 ms; Fig. 4C). Consistent with the MAP data in isolated hearts, MCT-induced prolongation of the QTc interval (236 ± 9.7 vs. 155 ± 7.1 ms) was significantly decreased in animals with PAH chronically treated with 0.5% RAN (198 ± 7.8 ms; Fig. 5A). ERP, which was increased in hearts from rats with PAH compared to sham (78 ± 3.5 vs. 51 ± 6.8 ms), was also normalized in hearts from rats with PAH treated with 0.5% RAN (54 ± 6.6 ms; Fig. 5B). Treatment with 0.5% RAN in sham animals had no (significant) effect on any of these electrophysiological parameters measured.

Effect of Chronic Administration of Ranolazine on Arrhythmogenesis in Hearts Isolated from Rats with PAH. The effect of RAN on the pro-arrhythmic potential of PAH was determined using isolated hearts from rats treated with vehicle or 0.5% RAN at 4 weeks following the injection of MCT. Burst pacing for 1 s at 50 Hz induced VT/VF in 50% of hearts isolated from rats with PAH (3 out of 6 hearts). In contrast, VT/VF was not inducible in hearts isolated from RAN treated rats ($P = 0.2$) and was only induced in 1 out of 6 hearts isolated from sham animals (Fig. 6A). Representative tracings of MAP, ECG, and LVP during arrhythmia induction are shown in figure 6B, C. Tracings from hearts isolated from sham and RAN-treated animals with PAH show that the hearts returned to normal sinus rhythm and function almost immediately after burst pacing, a triggered VF episode is evident in tracings from a heart of a rat with PAH without RAN (Fig. 6B, C).

Downloaded from jpet.aspetjournals.org at ASPET Journals on December 28, 2024

JPET Fast Forward. Published on March 13, 2015 as DOI: 10.1124/jpet.114.221861
This article has not been copyedited and formatted. The final version may differ from this version.

Acute Effect of Ranolazine on Arrhythmogenesis in PAH Rats and Isolated Hearts. Both *in vivo* and *ex vivo* experiments were conducted in order to determine the effect of acute administration of RAN on arrhythmia induction in the setting of established RV remodeling (Table 2), and these data are summarized in figure 7. Of note, hemodynamics were continually measured to ensure that no changes occurred with the doses of RAN used in these studies. In anesthetized rats with PAH arrhythmias were induced by a bolus injection of ISO (0.1 mg/kg, i.v.; Fig. 7A). Administration of ISO to animals with established PAH caused VT/VF and subsequent death in 70% of animals (7 out of 10), whereas ISO induced arrhythmias in only 17% of sham animals (1 out of 6). Furthermore, RAN (8 mg/kg bolus, 10 mg/kg/h infusion, i.v.) given 10 minutes prior to the ISO challenge completely prevented ISO-induced arrhythmias and death (0 out of 5; P=0.026 vs. without RAN treatment; Fig. 7A). Figure 7B shows representative tracings of PAP, BP, and ECG in a rat with PAH 6 minutes after an ISO injection that triggered VF.

Similar results were obtained in hearts isolated from rats at day 28 following the administration of MCT (PAH) when VT/VF was triggered using burst pacing for 1 s at 50 Hz. A total of 3 out of 6 hearts from the PAH group exhibited VT/VF. The electrical stimulation protocol provoked arrhythmias in 2 hearts while one heart exhibited spontaneous VT/VF prior to the electrical stimulation protocol. Acute administration of RAN (10 μM) 10 minutes prior to the burst stimulus completely prevented the induction of VT/VF (0 out of 10) in hearts from rats with PAH (P = 0.09 vs. without RAN treatment; Fig. 7C). In the sham group, the same stimulation protocol induced arrhythmias in 2 out of 11 hearts (18%). Representative tracings of MAP, ECG, and LV pressure from one RAN treated PAH heart are shown in figure 7D.

Downloaded from jpet.aspetjournals.org at ASPET Journals on December 28, 2024

JPET Fast Forward. Published on March 13, 2015 as DOI: 10.1124/jpet.114.221861
This article has not been copyedited and formatted. The final version may differ from this version.

Taking all different experiments together, the VT/VF could not be induced in PAH rats treated chronically or acutely with RAN whereas 50-70% of the PAH rats in the absence of RAN developed provoked VT/VF.

Downloaded from jpet.aspetjournals.org at ASPET Journals on December 28, 2024

JPET Fast Forward. Published on March 13, 2015 as DOI: 10.1124/jpet.114.221861
This article has not been copyedited and formatted. The final version may differ from this version.

Discussion

The present study shows that chronic treatment with RAN reduces maladaptive structural and electrical remodeling of the RV and prevents triggered ventricular arrhythmias in MCT-induced PAH in rats. Chronic administration of RAN initiated one week after the injection of MCT led to decreased RV hypertrophy and improved pulmonary hemodynamics in a dose-dependent manner. Circulating levels of BNP, a clinically validated biomarker of RV failure, were also significantly decreased in rats treated with RAN, indicating improved RV function (McLaughlin et al., 2013). Hearts isolated from rats with PAH showed a 50% induction in ES-induced VT/VF, whereas arrhythmia was not inducible in hearts isolated from PAH rats treated with RAN (acute and chronic). Furthermore, the prolonged APD, ERP, and QTc intervals measured in the RV of animals with PAH were significantly reduced following chronic RAN treatment. *In vivo* studies using rats with already established PAH and RV remodeling, demonstrated that the acute administration of RAN significantly reduced ISO-induced VT/VF and associated cardiovascular death. The results from these *in vivo* and *ex vivo* (isolated heart) experiments support that RAN reduces the arrhythmogenic substrate formation in the RV presumably by decreasing electrical heterogeneity (reduced RV-LV APD dispersion) and by decreasing cardiac fibrosis (structural remodeling), which results in an overall improvement in the electrical properties of the RV.

The Effect of Ranolazine on RV Structural and Functional Remodeling in Rats with PAH. The present understanding of maladaptive ventricular remodeling was established in experimental and human studies of left-heart failure, however, many of the same mechanisms have now been described in right-heart failure (Borgdorff et al., 2013; Simon, 2013).

Downloaded from jpet.aspetjournals.org at ASPET Journals on December 28, 2024

JPET Fast Forward. Published on March 13, 2015 as DOI: 10.1124/jpet.114.221861
This article has not been copyedited and formatted. The final version may differ from this version.

Importantly however, there are prominent embryological, structural, and metabolic differences which preclude the extrapolation of data between the two ventricles (Bogaard et al., 2009; Simon, 2013).

The current study was designed to investigate the effect of chronic treatment with RAN in an animal model of PAH that led to RV remodeling, electrical abnormalities, and failure. A significant increase in pulmonary arterial pressure following MCT injection was accompanied by RV hypertrophy, increased RV fibrosis, and impaired RV performance when compared to sham animals (Fig. 1-3). In the RV of rats with PAH, RAN dose-dependently slowed the development of ventricular hypertrophy and normalized the expression of collagen, CTGF, and TGF-β (Fig. 1 and 3). Additionally, in hearts isolated from rats with PAH, cardiac performance of the RV was normalized by RAN treatment (Table 1, supplemental data). The results of the current study evaluating the effects of chronic treatment with RAN are in good agreement with the results from a small clinical study evaluating RAN in patients with PAH (Shah et al., 2012), and with the recent report that RAN prevents MCT-induced pulmonary hypertension, RV hypertrophy, and RV fibrosis (Rocchetti et al., 2014). Our results are also consistent with the study conducted by Fang et al. demonstrating that RAN treatment improves RV performance as measured by exercise capacity and cardiac index in rats subjected to RV pressure overload by pulmonary artery banding (Fang et al., 2011).

BNP, a well-characterized biomarker that is predictive of RV performance, mortality, and clinical outcomes in patients with PAH (Sztrymf et al., 2010; McLaughlin et al., 2013; Vonk-Noordegraaf et al., 2013), was significantly increased in rats with PAH and was decreased by

Downloaded from jpet.aspetjournals.org at ASPET Journals on December 28, 2024

JPET Fast Forward. Published on March 13, 2015 as DOI: 10.1124/jpet.114.221861
This article has not been copyedited and formatted. The final version may differ from this version.

0.5% RAN (Fig. 1C). BNP is produced by and released from ventricular cardiomyocytes (Bruneau et al., 1997) and plasma levels of BNP are closely linked to the severity of ventricular remodeling and dysfunction (Sztrymf et al., 2010; McLaughlin et al., 2013). The effect of RAN to reduce BNP in our study is consistent with the benefits of RAN in animal models of left-heart disease, and with the amelioration of RV failure in this animal model (Aistrup et al., 2013; Guihaire et al., 2013; McLaughlin et al., 2013).

The Effect of Ranolazine on RV Electrical Remodeling in Rats with PAH. Cardiac arrhythmias are major contributors to morbidity and mortality in patients with PAH, can contribute to deteriorations of cardiac function, and are not adequately addressed by current therapies (Rajdev et al., 2012; Rich et al., 2013). Importantly, a recent prospective clinical study reported that the restoration of sinus rhythm using antiarrhythmic therapy was associated with a reduction in circulating BNP levels and improved survival (Olsson et al., 2013).

In the current study, the hearts from rats that received MCT had electrophysiological changes in the RV that were pro-arrhythmic (e.g. prolongation of QTc interval and heterogeneity of APD), and that had been reported in humans with PAH (Rajdev et al., 2012; Rich et al., 2013; Tanaka et al., 2013). As shown in figures 4 and 5, chronic treatment with RAN reduced the PAH-associated electrophysiological abnormalities. Additionally, ventricular heterogeneity in repolarization (RV-LV APD_{90}), a major contributor to the electrophysiological substrate (i.e. re-entry) leading to the occurrence of lethal arrhythmias, was also decreased by RAN.

Downloaded from jpet.aspetjournals.org at ASPET Journals on December 28, 2024

JPET Fast Forward. Published on March 13, 2015 as DOI: 10.1124/jpet.114.221861
This article has not been copyedited and formatted. The final version may differ from this version.

It was recently demonstrated that the preventative administration of RAN blocks late I_{Na} enhancement in RV myocytes and partially prevents the initiation of MCT-induced RV remodeling (Rocchetti et al., 2014). In that study, RAN administration was associated with improvements in Ca^{2+} handling, decreases in T-tubule disarray, and reduced incidence of delayed afterdepolarizations in RV myocytes (Rocchetti et al., 2014). Our data extend these findings by demonstrating that treatment with RAN decreases the pro-arrhythmic substrate of the remodeled RV and results in decreased incidences of provoked arrhythmias and protection from ISO-induced VT/VF. The present results from studies of chronic and acute RAN treatment in a model of RV dysfunction are also consistent with the well described anti-arrhythmic effects of RAN (Aistrup et al., 2013; Shryock et al., 2013) and support the therapeutic strategy of normalizing QTc interval and APD in order to reduce the arrhythmogenesis of diseased hearts.

Although reports of documented VT/VF are relatively rare in patients with PAH (approximately 8%) when compared to the reported incidence of bradycardia (45%), electromechanical dissociation (28%), and asystole (15%); VT/VF remains a clinically relevant risk for many patients with PAH (Hoeper et al., 2002; Vonk-Noordegraaf et al., 2013). In the current study a higher susceptibility to provoked VT/VF was observed *in vivo* (induced in 70%) and in isolated hearts from rats with PAH (induced in 50%) compared to normal hearts (induced in approximately 18%; Fig. 6). VT/VF inducibility was not observed with chronic RAN treatment and was prevented by acute administration of RAN to animals with established RV remodeling (Fig. 7A,B). Of note, a single incident of sudden cardiac death due to an episode of spontaneous VT/VF was captured during telemetric recording in a conscious rat several weeks following the injection of MCT (supplemental data). These data are in good agreement with Benoist et al. who

Downloaded from jpet.aspetjournals.org at ASPET Journals on December 28, 2024

JPET Fast Forward. Published on March 13, 2015 as DOI: 10.1124/jpet.114.221861
This article has not been copyedited and formatted. The final version may differ from this version.

demonstrated that MCT administration resulted in a higher incidence of provoked arrhythmias and sustained VT/VF compared to normal rat hearts (Benoist et al. 2011).

Limitations. Late I_{Na} was not directly measured in the current study, however, there is extensive clinical and experimental evidence to support late I_{Na} inhibition as the primary mechanism for the cardioprotective effects of RAN (Maier et al., 2013; Shryock et al., 2013). Notably, Rocchetti et al. recently demonstrated that late I_{Na} is enhanced in the RV of MCT rats and blocked by RAN (Rocchetti et al., 2014). In addition to inhibiting late I_{Na}, RAN has been reported to inhibit adrenergic receptors and to partially inhibit fatty acid oxidation at high concentrations (>100 μM; Minotti et al., 2013). Although these mechanisms cannot be completely excluded, it is unlikely that they are major contributors to the efficacy of RAN in MCT-induced PAH, as the plasma levels of RAN achieved in the present study have been shown to selectively inhibit late I_{Na} versus all other targets (Hale et al., 2008; Zhao et al., 2011). Of note, steady-state plasma levels of RAN (≤10 μM) had no effect on ISO-induced increases in heart rate in our acute studies indicating the lack of anti-adrenergic effects.

Conclusions. In the present study RAN, an anti-anginal, anti-ischemic drug known to have beneficial effects in models of LV dysfunction, was efficacious in reducing both structural and electrical remodeling of the RV in an animal model of PAH. In *in vivo* experiments, chronic administration of RAN dose-dependently decreased pulmonary artery pressure, RV hypertrophy, RV dysfunction, and the expression of fibrosis markers (collagen 1α1, CTGF and TGF-β) in the RV. These findings were supported with *ex vivo* experiments showing that RAN decreased electrical remodeling of the RV, as indicated by reduced repolarization abnormalities and by

Downloaded from jpet.aspetjournals.org at ASPET Journals on December 28, 2024

JPET Fast Forward. Published on March 13, 2015 as DOI: 10.1124/jpet.114.221861
This article has not been copyedited and formatted. The final version may differ from this version.

decreases in the prolonged ERP and QTc intervals. In *in vivo* experiments we showed that acute RAN treatment prevented triggered arrhythmias in hearts of rats with PAH (Fig. 7). In conclusion, the administration of RAN during PAH development decreased adverse structural remodeling and reduced the electrophysiological abnormalities of the diseased RV, providing evidence that the inhibition of late I_{Na} may have beneficial effects in the setting of RV impairment due to PAH.

Downloaded from jpet.aspetjournals.org at ASPET Journals on December 28, 2024

JPET Fast Forward. Published on March 13, 2015 as DOI: 10.1124/jpet.114.221861
This article has not been copyedited and formatted. The final version may differ from this version.

Acknowledgement

The authors gratefully acknowledge the expert assistance of Dr. Sarah Fernandes with the telemetry study.

Downloaded from jpet.aspetjournals.org at ASPET Journals on December 28, 2024

JPET Fast Forward. Published on March 13, 2015 as DOI: 10.1124/jpet.114.221861
This article has not been copyedited and formatted. The final version may differ from this version.

Authorship Contributions

Participated in research design: Hoyer, Liles, Chi, Dhalla, and Belardinelli.

Conducted experiments: Liles, Hoyer, and Oliver.

Performed data analysis: Hoyer, Liles, and Oliver.

Wrote or contributed to the writing of the manuscript: Liles, Hoyer, Chi, Dhalla, and Belardinelli.

Downloaded from jpet.aspetjournals.org at ASPET Journals on December 28, 2024

JPET Fast Forward. Published on March 13, 2015 as DOI: 10.1124/jpet.114.221861
This article has not been copyedited and formatted. The final version may differ from this version.

References

Abraham T, Wu G, Vastey F, Rapp J, Saad N, and Balmir E (2010) Role of combination therapy in the treatment of pulmonary arterial hypertension. *Pharmacotherapy* **30**:390-404.

Aistrup GL, Gupta DK, Kelly JE, O'Toole MJ, Nahhas A, Chirayil N, Misener S, Beussink L, Singh N, Ng J, Reddy M, Mongkolrattanothai T, El-Bizri N, Rajamani S, Shryock JC, Belardinelli L, Shah SJ, and Wasserstrom JA (2013) Inhibition of the late sodium current slows t-tubule disruption during the progression of hypertensive heart disease in the rat. *Am J Physiol* **305**:H1068-H1079.

Antzelevitch C, Nesterenko V, Shryock JC, Rajamani S, Song Y, and Belardinelli L (2014) The role of late I Na in development of cardiac arrhythmias. *Handb Exp Pharmacol* **221**:137-168.

Archer SL, Fang YH, Ryan JJ, and Piao L (2013) Metabolism and bioenergetics in the right ventricle and pulmonary vasculature in pulmonary hypertension. *Pulm Circ* **3**:144-152.

Benoist D, Stones R, Drinkhill M, Bernus O, and White E (2011) Arrhythmogenic substrate in hearts of rats with monocrotaline-induced pulmonary hypertension and right ventricular hypertrophy. *Am J Physiol* **300**:H2230-H2237.

Benoist D, Stones R, Drinkhill MJ, Benson AP, Yang Z, Cassan C, Gilbert SH, Saint DA, Cazorla O, Steele DS, Bernus O, and White E (2012) Cardiac arrhythmia mechanisms in rats with heart failure induced by pulmonary hypertension. *Am J Physiol* **302**:H2381-H2395.

Bogaard HJ, Abe K, Vonk Noordegraaf A, and Voelkel NF (2009) The right ventricle under pressure: cellular and molecular mechanisms of right-heart failure in pulmonary hypertension. *Chest* **135**:794-804.

Downloaded from jpet.aspetjournals.org at ASPET Journals on December 28, 2024

JPET Fast Forward. Published on March 13, 2015 as DOI: 10.1124/jpet.114.221861
This article has not been copyedited and formatted. The final version may differ from this version.

Borgdorff MA, Bartelds B, Dickinson MG, Steendijk P, and Berger RM (2013) A cornerstone of heart failure treatment is not effective in experimental right ventricular failure. *Int J Cardiol* **169**:183-189.

Bruneau BG, Piazza LA, and de Bold AJ (1997) BNP gene expression is specifically modulated by stretch and ET-1 in a new model of isolated rat atria. *Am J Physiol* 273:H2678-H2686.

Bruner LH, Hilliker KS, and Roth RA. (1983) Pulmonary hypertension and ECG changes from monocrotaline pyrrole in the rat. *Am J Physiol* **245**:H300-H306.

Fang YH, Piao L, Hong Z, Toth PT, Marsboom G, Bache-Wiig P, Rehman J, and Archer SL (2012) Therapeutic inhibition of fatty acid oxidation in right ventricular hypertrophy: exploiting Randle's cycle. *J Mol Med* **90**:31-43.

Freund-Michel V, Guibert C, Dubois M, Courtois A, Marthan R, Savineau JP, and Muller B (2013) Reactive oxygen species as therapeutic targets in pulmonary hypertension. *Ther Adv Respir Dis* **7**:175-200.

Guihaire J, Bogaard HJ, Flecher E, Noly PE, Mercier O, Haddad F, and Fadel E (2013) Experimental models of right heart failure: a window for translational research in pulmonary hypertension. *Semin Respir Crit Care Med* **34**:689-699.

Hale SL, Shryock JC, Belardinelli L, Sweeney M, and Kloner RA (2008) Late sodium current inhibition as a new cardioprotective approach. *J Mol Cell Cardiol* **44**:954-967.

Hoeper MM, Galie N, Simonneau G, and Rubin LJ (2002) New treatments for pulmonary arterial hypertension. *Am J Respir Crit Care Med* **165**:1209-1216.

Hoorn CM and Roth RA (1992) Monocrotaline pyrrole alters DNA, RNA and protein synthesis in pulmonary artery endothelial cells. *Am J Physiol* **262**:L740-L747.

Downloaded from jpet.aspetjournals.org at ASPET Journals on December 28, 2024

JPET Fast Forward. Published on March 13, 2015 as DOI: 10.1124/jpet.114.221861
This article has not been copyedited and formatted. The final version may differ from this version.

Lappin PB and Roth RA (1997) Hypertrophy and prolonged DNA synthesis in smooth musclecells characterize pulmonary arterial wall thickening after monocrotaline pyrrole administration to rat. J *Toxicol Pathol* **25**:372-380.

Maier LS, Layug B, Karwatowska-Prokopczuk E, Belardinelli L, Lee S, Sander J, Lang C, Wachter R, Edelmann F, Hasenfuss G, and Jacobshagen C (2013) RAnoLazIne for the treatment of diastolic heart failure in patients with preserved ejection fraction: the RALI-DHF proof-of-concept study. *JACC Heart failure* **1**:115-122.

Malenfant S, Margaillan G, Loehr JE, Bonnet S, and Provencher S (2013) The emergence of new therapeutic targets in pulmonary arterial hypertension: from now to the near future. *Expert Rev Respir Med* **7**:43-55.

McLaughlin VV, Gaine SP, Howard LS, Leuchte HH, Mathier MA, Mehta S, Palazzini M, Park MH, Tapson VF, and Sitbon O (2013) Treatment goals of pulmonary hypertension. *J Am Coll Cardiol*. 2013 **62(**25 Suppl):D73-D81.

Olsson KM, Nickel NP, Tongers J, and Hoeper MM (2013) Atrial flutter and fibrillation in patients with pulmonary hypertension. *Int J Cardiol* **167**:2300-2305.

Rain S, Handoko ML, Trip P, Gan CT, Westerhof N, Stienen GJ, Paulus WJ, Ottenheijm CA, Marcus JT, Dorfmuller P, Guignabert C, Humbert M, Macdonald P, Dos Remedios C, Postmus PE, Saripalli C, Hidalgo CG, Granzier HL, Vonk-Noordegraaf A, van der Velden J, and de Man FS (2013) Right ventricular diastolic impairment in patients with pulmonary arterial hypertension. *Circulation* **128**:2016-2025.

Rain S, Handoko ML, Vonk Noordegraaf A, Bogaard HJ, van der Velden J, and de Man FS (2014) Pressure-overload-induced right heart failure. *Pflugers Arch* **466**:1055-1063.

Downloaded from jpet.aspetjournals.org at ASPET Journals on December 28, 2024

JPET Fast Forward. Published on March 13, 2015 as DOI: 10.1124/jpet.114.221861
This article has not been copyedited and formatted. The final version may differ from this version.

Rajdev A, Garan H, and Biviano A (2012) Arrhythmias in pulmonary arterial hypertension. *Prog Cardiovasc Dis* **55**:180-186.

Rastogi S, Sharov VG, Mishra S, Gupta RC, Blackburn B, Belardinelli L, Stanley WC, and Sabbah HN (2008) Ranolazine combined with enalapril or metoprolol prevents progressive LV dysfunction and remodeling in dogs with moderate heart failure. *Am J Physiol* **295**:H2149-H2155.

Rich JD, Thenappan T, Freed B, Patel AR, Thisted RA, Childers R, and Archer SL (2013) QTc prolongation is associated with impaired right ventricular function and predicts mortality in pulmonary hypertension. *Int J Cardiol* **167**:669-676.

Rocchetti M, Sala L, Rizzetto R, Staszewsky LI, Alemanni M, Zambelli V, Russo I, Barile L, Cornaghi L, Altomare C, Ronchi C, Mostacciuolo G, Lucchetti J, Gobbi M, Latini ,R and Zaza A (2014) Ranolazine prevents INaL enhancement and blunts myocardial remodelling in a model of pulmonary hypertension. *Cardiovasc Res* **104**:37-48.

Rosenberg HC and Rabinovitch M (1988) Endothelial injury and vascular reactivity in monocrotaline pulmonary hypertension. *Am J Physiol*. **255**:H1484 –H1491.

Shah SJ, Cuttica MJ, Beussink L, Mkrdichian H, Samari R, Benefield B, Selvaraj S, DeMatte JE, and Lee DC (2012) A pilot study of the effects of ranolazine on right ventricular structure and function, exercise capacity, and symptoms in pulmonary arterial hypertension. *Circulation* **126:**A18974.

Shryock JC, Song Y, Rajamani S, Antzelevitch C, and Belardinelli L (2013) The arrhythmogenic consequences of increasing late INa in the cardiomyocyte. *Cardiovasc Res* **99**:600-611.

Simon MA (2013) Assessment and treatment of right ventricular failure. *Nat Rev Cardiol* **10**:204-218.

Downloaded from jpet.aspetjournals.org at ASPET Journals on December 28, 2024

JPET Fast Forward. Published on March 13, 2015 as DOI: 10.1124/jpet.114.221861
This article has not been copyedited and formatted. The final version may differ from this version.

Sztrymf B, Souza R, Bertoletti L, Jais X, Sitbon O, Price LC, Simonneau G, and Humbert M (2010) Prognostic factors of acute heart failure in patients with pulmonary arterial hypertension. *Eur Resp J* **35**:1286-1293.

Tanaka Y, Takase B, Yao T, and Ishihara M (2013) Right ventricular electrical remodeling and arrhythmogenic substrate in rat pulmonary hypertension. *Am J Resp Cell Mol Biol* **49**:426-436.

Toischer K, Hartmann N, Wagner S, Fischer TH, Herting J, Danner BC, Sag CM, Hund TJ, Mohler PJ, Belardinelli L, Hasenfuss G, Maier LS, and Sossalla S (2013) Role of late sodium current as a potential arrhythmogenic mechanism in the progression of pressure-induced heart disease. *J Mol Cell Cardiol* **61**:111-122.

van de Veerdonk MC, Kind T, Marcus JT, Mauritz GJ, Heymans MW, Bogaard HJ, Boonstra A, Marques KM, Westerhof N, and Vonk-Noordegraaf A (2011) Progressive right ventricular dysfunction in patients with pulmonary arterial hypertension responding to therapy. *J Am Coll Cardiol* **58**:2511-2519.

Voelkel NF, Gomez-Arroyo J, Abbate A, Bogaard HJ, and Nicolls MR (2012) Pathobiology of pulmonary arterial hypertension and right ventricular failure. *Eur Respir J* **40**:1555-1565.

Vonk-Noordegraaf A, Haddad F, Chin KM, Forfia PR, Kawut SM, Lumens J, Naeije R, Newman J, Oudiz RJ, Provencher S, Torbicki A, Voelkel NF, and Hassoun PM (2013) Right heart adaptation to pulmonary arterial hypertension: physiology and pathobiology. *J Am Coll Cardiol* **62**:D22-D33.

Yin FC, Spurgeon HA, Rakusan K, Weisfeldt ML, and Lakatta EG (1982) Use of tibial length to quantify cardiac hypertrophy: application in the aging rat. *Am J Physiol* **243**:H941-H947.

Downloaded from jpet.aspetjournals.org at ASPET Journals on December 28, 2024

JPET Fast Forward. Published on March 13, 2015 as DOI: 10.1124/jpet.114.221861
This article has not been copyedited and formatted. The final version may differ from this version.

Zhao G, Walsh E, Shryock JC, Messina E, Wu Y, Zeng D, Xu X, Ochoa M, Baker SP, Hintze TH, and Belardinelli L (2011) Antiadrenergic and hemodynamic effects of ranolazine in conscious dogs. *J Cardiovasc Pharmacol* **57**:639-647.

Downloaded from jpet.aspetjournals.org at ASPET Journals on December 28, 2024

JPET Fast Forward. Published on March 13, 2015 as DOI: 10.1124/jpet.114.221861
This article has not been copyedited and formatted. The final version may differ from this version.

Footnotes

[#]J.T.L. and [#]K.H. equally contributed to this work and are considered co-first authors.

This project was supported by Gilead Sciences, Inc. J.T.L., K.H., J.O., L.C., A.D., and L.B. are employees of Gilead Sciences.

Downloaded from jpet.aspetjournals.org at ASPET Journals on December 28, 2024

JPET Fast Forward. Published on March 13, 2015 as DOI: 10.1124/jpet.114.221861
This article has not been copyedited and formatted. The final version may differ from this version.

Figure Legends

Figure 1. Effect of chronic administration of RAN to rats with PAH. At 4 weeks following MCT injection, the rats developed significant RV hypertrophy (**A**), increased RV developed pressure (**B**), and increased plasma BNP levels (**C**) compared to sham animals. Chronic administration of RAN starting 1 week after the injection of MCT dose-dependently decreased RV hypertrophy, RV developed pressure, and plasma BNP levels. Data are the mean ± S.E.M. (One-way ANOVA followed by Newman-Keuls post-hoc analysis with all pair-wise comparisons; n = 6-10). **P*<0.05 vs. sham; †*P*<0.05 vs. MCT; ‡*P*<0.05 vs. 0.25% RAN.

Figure 2. Effect of chronic administration of RAN to rats with MCT-induced PAH. Systolic (**A**), mean (**B**), and diastolic (**C**) pulmonary arterial pressures were measured at 4 weeks following MCT injection. PAH caused significant increases in systolic, mean, and diastolic pulmonary arterial pressures compared to control (sham) animals. One week following MCT injection two groups of rats were switched to a diet with either 0.25 or 0.5% RAN by weight, which dose-dependently decreased pulmonary arterial pressures. Data are the mean ± S.E.M. (One-way ANOVA followed by Newman-Keuls post-hoc analysis with all pair-wise comparisons; n = 6-10). **P*<0.05 vs. sham; †*P*<0.05 vs. MCT; ‡*P*<0.05 vs. 0.25% RAN.

Figure 3. Representative images of RV stained with Masson's Trichrome from sham (**A**), MCT + vehicle (**B**), and MCT + 0.5% RAN (**C**) at 4 weeks following the injection of MCT; fibrosis is colored blue (100x). RAN dose-dependently reduced the PAH-induced increases in mRNA expression of collagen1α1 (**D**), connective tissue growth factor (CTGF; **E**), and TGF-β (**F)** in the

Downloaded from jpet.aspetjournals.org at ASPET Journals on December 28, 2024

JPET Fast Forward. Published on March 13, 2015 as DOI: 10.1124/jpet.114.221861
This article has not been copyedited and formatted. The final version may differ from this version.

RV. Data are the mean ± S.E.M. (One-way ANOVA followed by a Bonferroni multiple comparisons test; n = 5-9). *P<0.05 vs. sham; $^{\dagger}P$<0.05 vs. MCT; $^{\ddagger}P$<0.05 vs. 0.25% RAN.

Figure 4. Effect of chronic administration of RAN on the monophasic action potential (MAP) and repolarization abnormalities in the RV of isolated hearts from rats with PAH. Superimposed MAPs of hearts from sham (blue), PAH (black), and PAH + 0.5% RAN (red) animals showing differences in MAP duration (**A**). RV MAP duration at 30, 50 and 90% repolarization was significantly prolonged in hearts from rats with PAH and reduced with 0.5% RAN (0.5% Ran by weight in chow) treatment (n = 5-6; **B**). Electrical heterogeneity defined as interventricular dispersion (RV-LV APD_{90}) was significantly increased in hearts from rats with PAH and normalized with chronic 0.5% RAN treatment when compared to isolated hearts from normal (sham) rats (n = 5-6; **C**). Data are the mean ± S.E.M. (One-way ANOVA followed by Tukey post-hoc analysis with all pair-wise comparisons). *P<0.05 vs. sham; $^{\dagger}P$<0.05 vs. MCT.

Figure 5. Effect of chronic administration of RAN on electrophysiological parameters. In isolated hearts from rats with PAH, surface ECG revealed prolonged QTc interval calculated according to the Bazett formula (n = 6 in all groups; **A**) and increased effective refractory period (ERP; n = 4-6; **B**) compared to normal hearts. Chronic 0.5% RAN treatment, which began at 1 week after the injection of MCT, showed decreased QTc interval and normalized ERP values at 4 weeks post MCT injection. Data are the mean ± S.E.M. (One-way ANOVA followed by Tukey post-hoc analysis with all pair-wise comparisons). *P<0.05 and **P<0.02 vs. sham; $^{\dagger}P$<0.05 vs. MCT.

Downloaded from jpet.aspetjournals.org at ASPET Journals on December 28, 2024

JPET Fast Forward. Published on March 13, 2015 as DOI: 10.1124/jpet.114.221861
This article has not been copyedited and formatted. The final version may differ from this version.

Figure 6. Effect of chronic administration of RAN on electrical stimulation-induced arrhythmias in isolated hearts from rats with PAH (4 weeks after the injection of MCT). Summarized data of incidences of VT/VF triggered by burst pacing in hearts isolated from normal, PAH, or PAH + 0.5% RAN ($P = 0.2$, Fisher's Exact test; **A**). Representative tracings of RV monophasic action potential (MAP), ECG, left-ventricular pressure (LVP), and of electrical stimulation depicted before, during, and after burst pacing (1 s, 50 Hz) experiments in isolated hearts from rats with PAH (**B**) and rats with PAH treated with 0.5% RAN in diet by weight (**C**).

Figure 7. Acute administration of RAN *in vivo* prevents triggered VT/VF in hearts from rats with PAH. Summary data of VT/VF incidences and subsequent sudden cardiac death in rats with PAH in the presence or absence of RAN (8 mg/kg bolus, followed by 10 mg/kg/h infusion, i.v.) are shown (*$P < 0.03$ vs. PAH only, Fisher's Exact test). The administration of isoproterenol (ISO, 0.1 mg/kg, i.v.) to rats with established PAH caused VT/VF (**A**). Depicted are representative tracings of pulmonary arterial pressure (PAP), systemic blood pressure (BP), and ECG at 7 min following an ISO bolus injection (0.1 mg/kg, i.v.) inducing VF in a rat with PAH (*in vivo*, **B**). Summary data of incidences of VT/VF in the absence or presence of 10 μM RAN are shown for *ex vivo* experiments. VT/VF was electrically triggered by burst pacing (1 s, 50 Hz). In the PAH group, one heart exhibited spontaneous VT/VF shown as grey in the black bar (**C**). Representative tracings of RV monophasic action potential (MAP), ECG, left-ventricular pressure (LVP), and electrical stimulation before, during, and after burst pacing in isolated hearts from rats with PAH perfused with 10 μM RAN are depicted (*ex vivo*, **D**).

Downloaded from jpet.aspetjournals.org at ASPET Journals on December 28, 2024

JPET Fast Forward. Published on March 13, 2015 as DOI: 10.1124/jpet.114.221861
This article has not been copyedited and formatted. The final version may differ from this version.

Table 1. Effect of chronic treatment with RAN on systemic blood pressure and heart rate in animals with MCT-induced PAH. Measurements were performed at 28 days after injection of MCT (60 mg/kg body weight). One week after MCT injection, two groups of rats were switched to a diet containing either 0.25 or 0.5% RAN by weight. **P*<0.05 vs. sham.

	Sham	**PAH**	**PAH + 0.25 % RAN**	**PAH + 0.5% RAN**
Mean Arterial Pressure (mmHg)	95 ± 6.9	89 ± 7.6*	100 ± 5.2	99 ± 1.7
Heart Rate (bpm)	291 ± 17	292 ± 12	313 ± 13	300 ± 21

Downloaded from jpet.aspetjournals.org at ASPET Journals on December 28, 2024

JPET Fast Forward. Published on March 13, 2015 as DOI: 10.1124/jpet.114.221861
This article has not been copyedited and formatted. The final version may differ from this version.

Table 2. Summary of pulmonary hemodynamics, RV hypertrophy, and heart rate (HR) data from animals subjected to isoproterenol (ISO) challenge. All rats with PAH had a similar PAH phenotype prior to the administration of ISO (0.1 mg/kg, i.v.). Of note, ISO induced similar increases in HR across groups. **P*<0.05 vs. sham.

	Sham	**PAH**
Baseline systolic pulmonary pressure (mmHg)	25 ± 4	41 ± 9*
RV hypertrophy (mg/mm)	6.7 ± 0.7	10.5 ± 2*
Baseline HR (bpm)	315 ± 55	280 ± 30*
Increase in HR following ISO challenge (bpm)	108 ± 28	96 ± 30

Downloaded from jpet.aspetjournals.org at ASPET Journals on December 28, 2024

JPET Fast Forward. Published on March 13, 2015 as DOI: 10.1124/jpet.114.221861
This article has not been copyedited and formatted. The final version may differ from this version.

1A

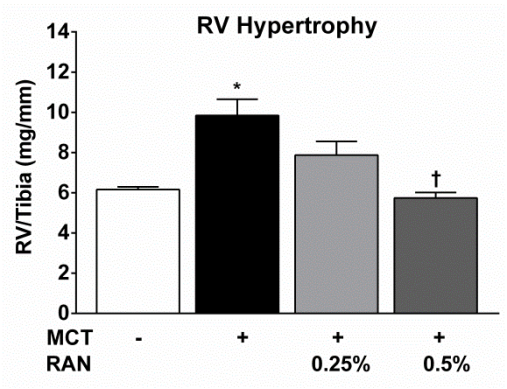

1B

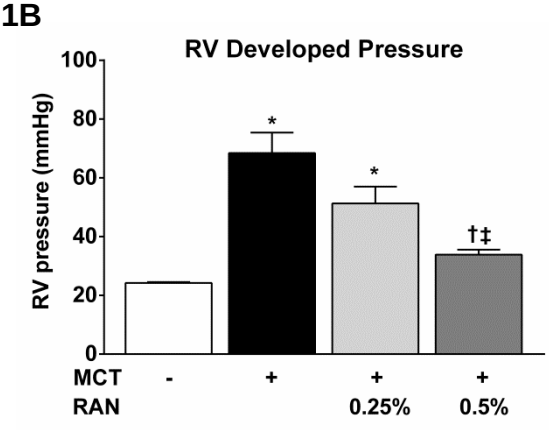

1C

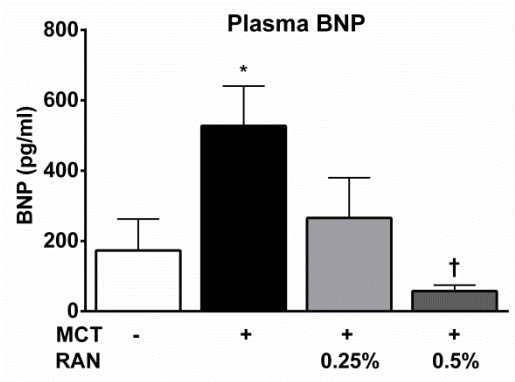

Figure 1

Downloaded from jpet.aspetjournals.org at ASPET Journals on December 28, 2024

JPET Fast Forward. Published on March 13, 2015 as DOI: 10.1124/jpet.114.221861
This article has not been copyedited and formatted. The final version may differ from this version.

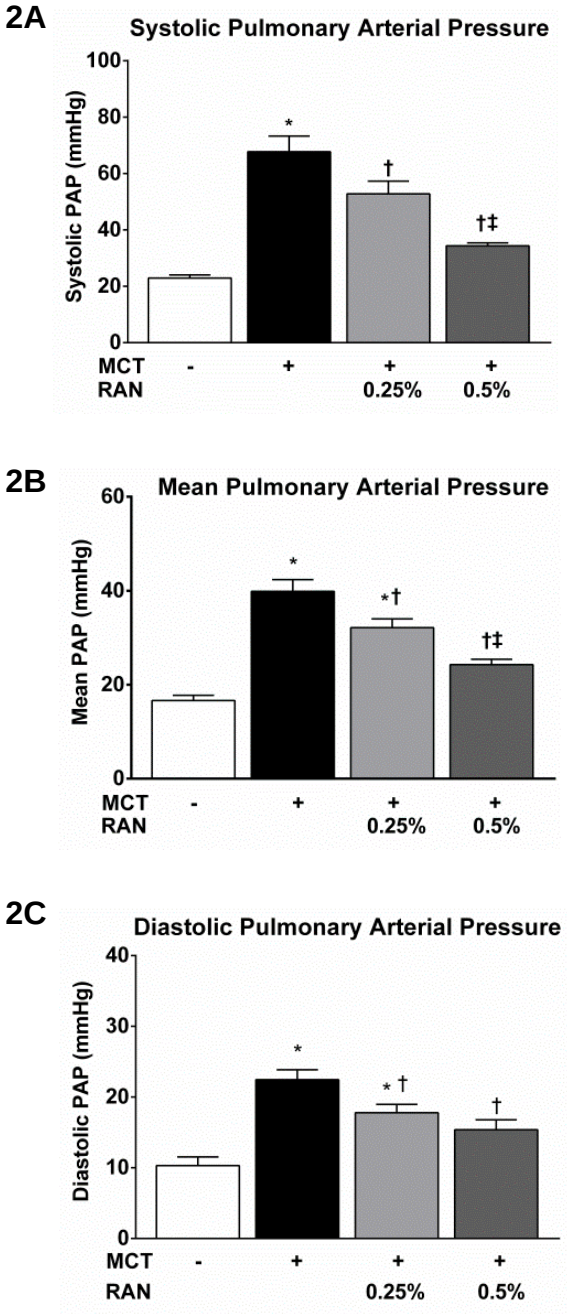

Figure 2

Downloaded from jpet.aspetjournals.org at ASPET Journals on December 28, 2024

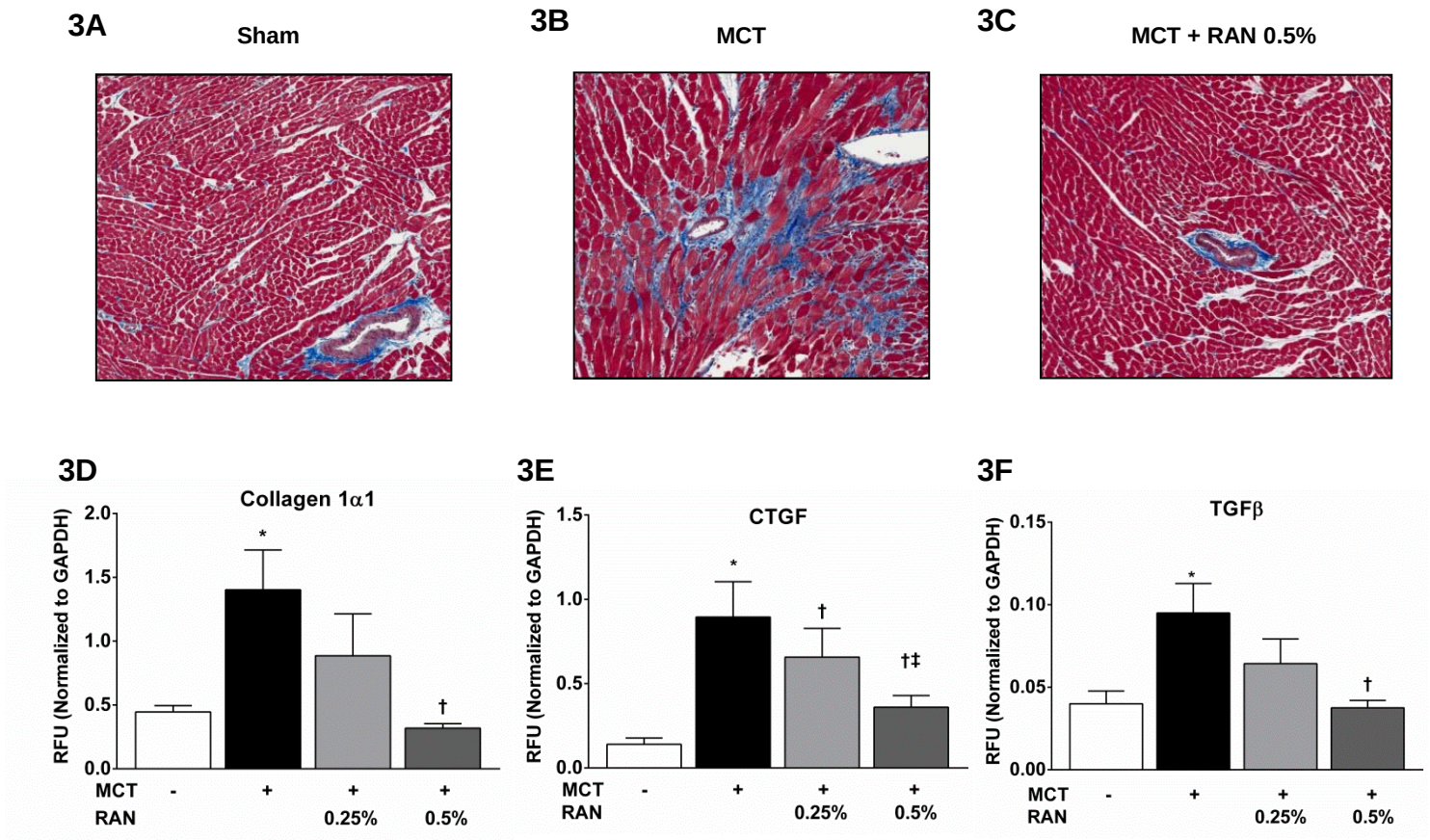

Figure 3

JPET Fast Forward. Published on March 13, 2015 as DOI: 10.1124/jpet.114.221861
This article has not been copyedited and formatted. The final version may differ from this version.

Downloaded from jpet.aspetjournals.org at ASPET Journals on December 28, 2024

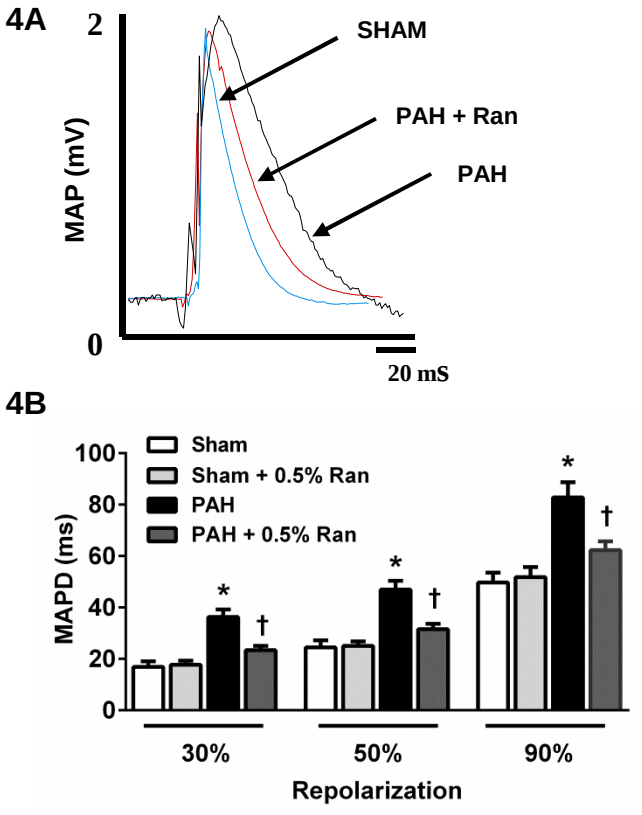

Figure 4

Downloaded from jpet.aspetjournals.org at ASPET Journals on December 28, 2024

JPET Fast Forward. Published on March 13, 2015 as DOI: 10.1124/jpet.114.221861
This article has not been copyedited and formatted. The final version may differ from this version.

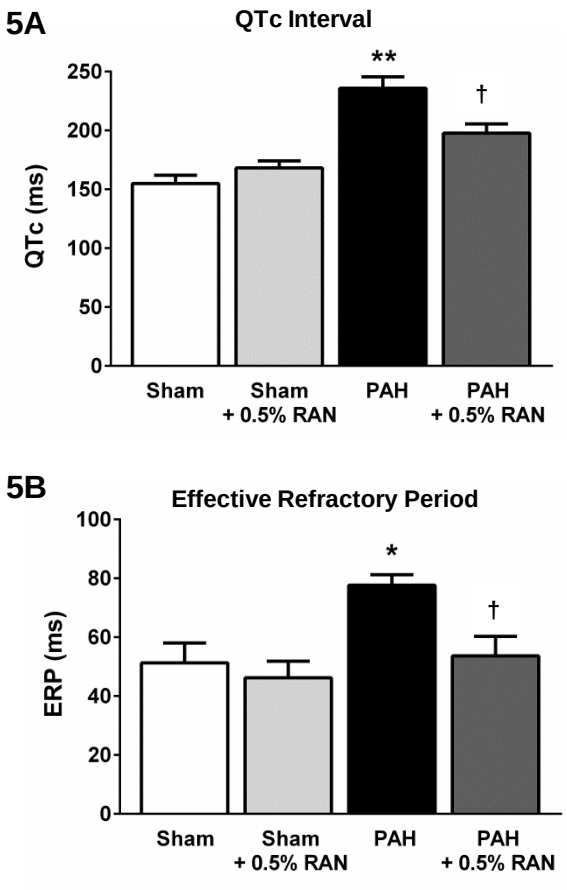

Figure 5

JPET Fast Forward. Published on March 13, 2015 as DOI: 10.1124/jpet.114.221861
This article has not been copyedited and formatted. The final version may differ from this version.

Downloaded from jpet.aspetjournals.org at ASPET Journals on December 28, 2024

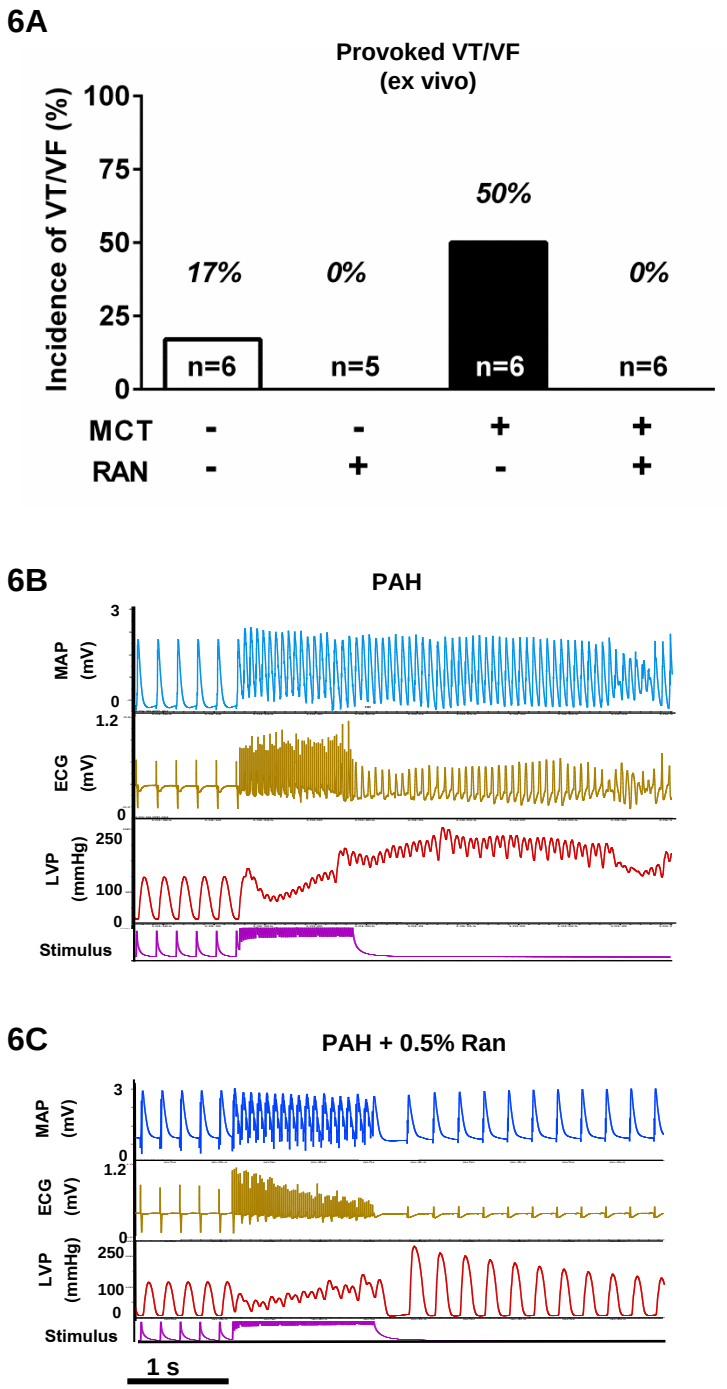
6A
Provoked VT/VF
(ex vivo)
Incidence of VT/VF (%)
100
75
50
25
0
17%
0%
50%
0%
n=6
n=5
n=6
n=6
MCT - - + +
RAN - + - +
6B
PAH
MAP (mV)
3
0
ECG (mV)
1.2
0
LVP (mmHg)
250
100
0
Stimulus
6C
PAH + 0.5% Ran
MAP (mV)
3
0
ECG (mV)
1.2
0
LVP (mmHg)
250
100
0
Stimulus
1 s

Figure 6

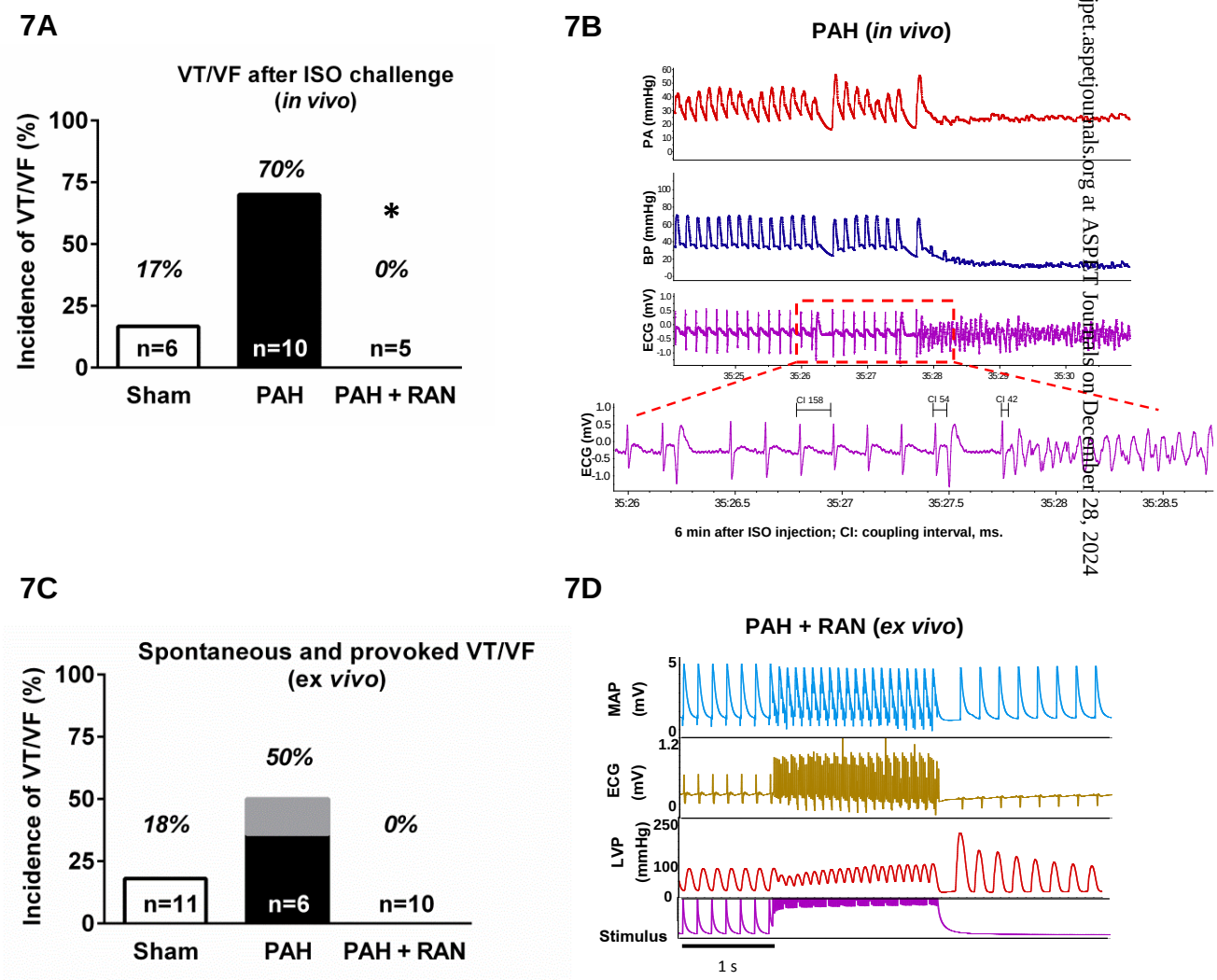

Figure 7

Downloaded from jpet.aspetjournals.org at ASPET Journals on December 28, 2024